Effect of High Gravity on Weld Fusion Zone Shape

With an increase in gravitational acceleration, the depth-to-width ratio of the weld fusion zone tends to decrease

BY D. K. AIDUN, J. J. DOMEY AND G. AHMADI

ABSTRACT. Understanding the physical phenomena involved in arc welding is of substantial value to improving the weldability of materials. One major factor affecting the motion within the weld pool is the gravity-driven buoyancy force. This force opposes the electromagnetic force-induced flow and opposes or enhances the Marangoni convective flow within the weld pool depending on the sign of the surface tension gradient ($d\gamma/dT$). Physical experiments for spot GTA welding of commercially pure nickel (Ni-270) in the high-gravity condition (1 g = 9.8 m/s² to 10 g = 98 m/s²) were conducted in the Multi-Gravity Research Welding System at Clarkson University. It was found the depth-to-width ratio (d/w) of the weld fusion zone decreases as the net acceleration increases to 10 g. In addition, a trace element of iron (Fe) was added to the spot GTA welds at various g levels to better visualize the weld fusion zone. This case also showed the d/w ratio of the fusion zone decreases with the increase in gravitational acceleration.

Introduction

In light of the safety, economic and environmental factors concerned, we need to pay more attention to the advancement of manufacturing and fabrication processes such as welding (Ref. 1).

Whether the welding processes are used on earth or in space, they have the same common objective: to obtain defect-free welds. A defect can be defined as a discontinuity that inhibits a weldment from meeting the desired specifications/code requirements and includes such items as porosity, hot cracking and incomplete penetration. To achieve this objective, reliable science-based correlations between the environment, welding process/technique, microstructure and properties of weldments, as well as models to predict such relations, must be developed.

To quantitatively understand the mechanisms behind defects in welds, one first has to examine and characterize the convection and heat transfer in weld pools and their effects on the overall weld integrity. Buoyancy, Marangoni and electromagnetic forces have been found to have significant effect on the fluid flow in arc weld pools (Refs. 2–14). In spite of the significant need for metal joining in different gravitational fields, the effect of gravity, especially high gravity, on the weld pool dynamics is not understood.

Keanini and Rubinsky (Ref. 15) studied plasma arc welding (PAW) of steel in a reduced-gravity environment. They reported that, for PAW, gravity did not have a significant effect on weld shape for their full-penetration welds. The major observed effect was pulling the weld downward, which widened the bottom of the pool. The authors also reported their results for the effects of gravity were independent of the mass flow rate of the plasma, initial temperature of the base metal and surface tension of the molten weld pool. Russell, *et al.* (Ref. 16), reviewed various weld processes being considered for use in the construction, repair and fabrication of metal structures for space applications. Kaukler and Workman (Ref. 17) proposed that laser welding can be a viable joining process for space construction. They conducted simulations using a laser beam welding system on board a NASA KC-135 aircraft. The specimen was kept in a vacuum chamber to more closely represent the space environment. They reported an increase in penetration on the welds performed in a microgravity environment at 0.1 g = 0.98 m/s² over those performed in the normal environment of 1 g = 9.8 m/s². Wang and Tandon (Ref. 18) studied the microstructure changes of laser beam welding thin sheets of 316 stainless steel in a reduced-gravity environment. They reported that reduced gravity caused both the width and depth of the weld pool to increase over similar welds performed at 1 g. They also noticed an increase in porosity and suspended weld particles in microgravity conditions, which may lead to a weaker weld joint. Domey, *et al.* (Ref. 19), numerically simulated spot GTA welds onto aluminum under different gravitational fields. They found the convective flow field in the weld pool in a low-gravity environment (<1 g) is governed by a combination of the electromagnetic force and the Marangoni force, while for normal 1-g and high-gravity 2-g environments, the weld pool convection is driven by the buoyancy force. Recently, Singh, Kang, Lambrakos and Marsh (Ref. 20) reported the weld pool geometry changes considerably depending on gravity and the width of the weld pool was observed to increase by about 10% at 1.8 g compared with the width at ~1.2 g.

The general scope of this work is to provide a better understanding of the role of enhanced buoyancy-driven flow at high g on the weld pool size and shape of GTA welds. A series of physical spot GTA welding of commercially pure

KEY WORDS

Gravitational Acceleration
Buoyancy Force
Electromagnetic Force
Marangoni Convective Flow
GTAW
Ni-270
Fusion Zone

D. K. AIDUN, J. J. DOMEY and G. AHMADI are with the Mechanical & Aeronautical Engineering Department, Clarkson University, Potsdam, N.Y.

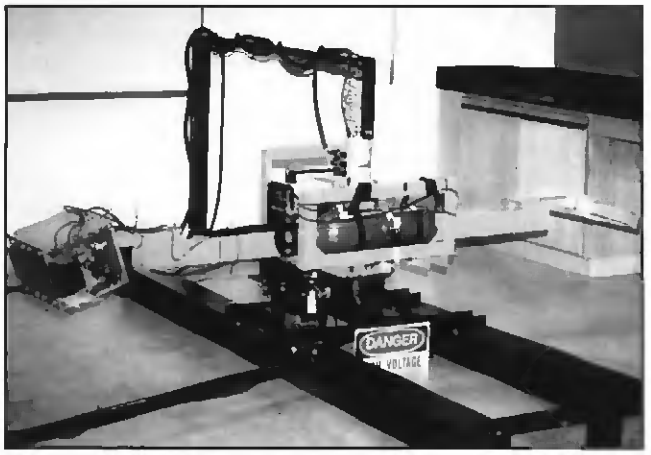

Fig. 1 — The Multi-Gravity Research Welding System (MGRWS) during rotation.

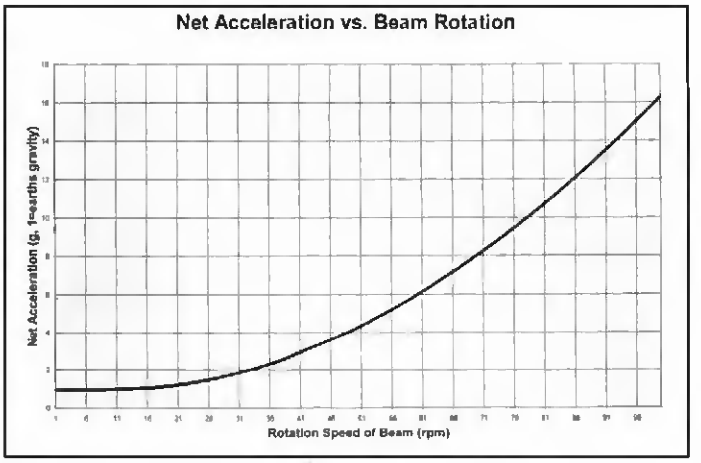

Fig. 2 — Net acceleration of the MGRWS as a function of the rotation rate (rpm).

Table 1 — Mill Composition of Ni-270

Element	Wt-%
Ni	99.95 min.
C	0.02 max.
Fe	0.005 max.
Mn, Cr, Ti, Mg, Co, Cu, Si, and S	0.001 max.

Table 2 — Spot GTA Welding Parameters for Ni-270 at 1, 5 and 10 g

Arc Voltage	16 volts
Arc Current	100 amps (DCEN)
Shielding Gas and Flow Rate	75Ar-25He and 1.0 m/h
Arc Length	1.0 mm
Electrode Extension	2.0 mm
Electrode, Size, Tip Angle and Orientation	W+2%ThO_2; 3.18 mm, 60 deg and 90 deg to the workpiece
Weld or Arc Time	10 seconds
Preheat	None

nickel for a range of high-gravity conditions in the Multi-Gravity Research Welding System (MGRWS) was performed. The variation of depth-to-width ratio as a function of gravity was studied. The effect of a trace element of iron was also analyzed.

High-Gravity Environment

To examine the effect of increased gravity (>1 g) on weld pool size and shape, a high-gravity environment was created using a centrifuge called the Multi-Gravity Research Welding System (MGRWS), which was designed and built at Clarkson University (Ref. 21). The MGRWS has a 1.15-m beam (arm) length and is capable of rotating at speeds in excess of 86 rpm (>12 g). Pictures of the MGRWS are shown in Figs. 1 and 2. The MGRWS is also capable of being outfitted with both the gas tungsten arc welding (GTAW) and gas metal arc welding (GMAW) processes. The welding box shown in Fig. 3 is pivoted so the net acceleration experienced is parallel to the torch and perpendicular to the bottom of the box at all times, as shown schematically in Fig. 4.

Regel and Wilcox (Ref. 22) discussed the changes that occur to a fluid when it is placed into a centrifuge with an arm length of r rotating at an angular velocity of ω. They noted that three major changes occur: 1) The net radial acceleration of the fluid is increased by $\omega^2 r$, where r is the radial distance; 2) a Coriolis acceleration of the form $2\omega \times v$ is introduced, where x represents the vector cross product and v is the local fluid velocity in the rotating frame; and 3) the acceleration vector varies in both direction and magnitude throughout the fluid due to the variation of r in the $\omega^2 r$ term. These terms are related to the net acceleration, Coriolis acceleration and acceleration gradient, respectively. The Coriolis force in this case acts perpendicular to the plane of Fig. 4, and its magnitude varies because of the change in the fluid velocity in the weld pool.

Experimental Procedures

Base Material

It is well known small variations in chemical composition can have dramatic effects on resulting welds. Therefore, commercially pure nickel (Ni-270) was chosen as the base metal for this investigation. The Ni-270 stock was provided in a 25.4-mm-diameter swaged bar. The composition of the nickel is shown in Table 1. Samples of nickel were sliced from the base stock to the final dimensions of 25.4 mm diameter by 3.18 mm thick. The "to be welded" surface was subjected to 320 SiC paper to provide a consistent surface finish for all of the samples.

Welding Parameters/Procedures

The samples were subjected to a spot GTA welding process using the MGRWS with the parameters shown in Table 2. The MGRWS was brought up to the desired speed (rpm) by remote control to obtain the specific g level. Once at the desired g level, the arc was turned on and the weld was performed for the predetermined arc time of 10 s. After completing the weld, the centrifuge was allowed to continue spinning for 60 s to allow for the initial cooling. Then the MGRWS was slowly brought to a stop using a foot brake.

The welded samples were then sectioned, polished and etched for metallographic analysis. The welds were photographed using a stereomicroscope with a magnification of 19.5X. The resulting photographs were digitally scanned using a 600 x 600 dots-per-inch scanner, producing accuracy to within 5 pixels or ± 5 microns. This technique was used for all the welds for determination of the depth (d) and width (w) of the fusion zones.

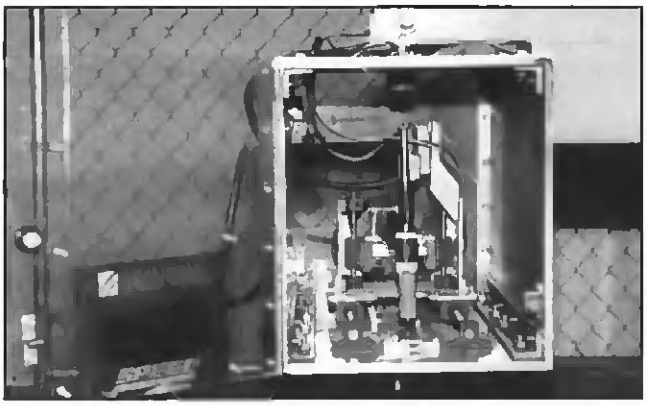

Fig. 3 — Welding box of the MGRWS.

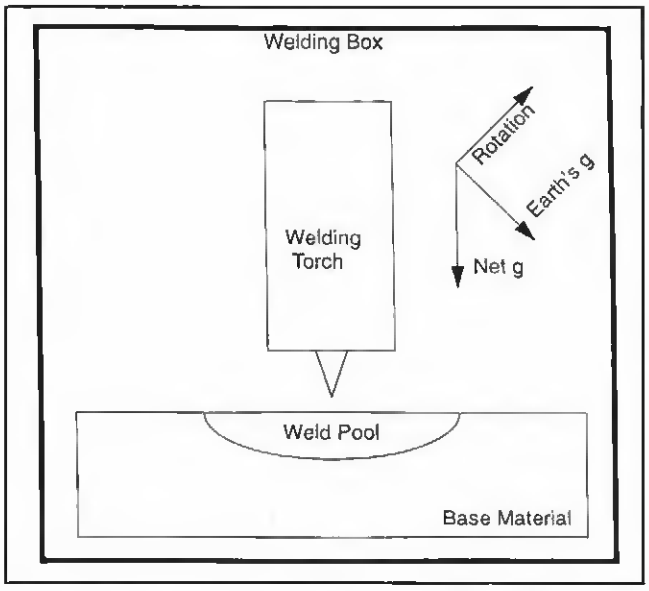

Fig. 4 — The orientation of the net acceleration with respect to the welding torch and the workpiece (see arrows).

Fig. 5 — The shape of the fusion zone of a Ni-270 GTA weld at 1 g (no rotation).

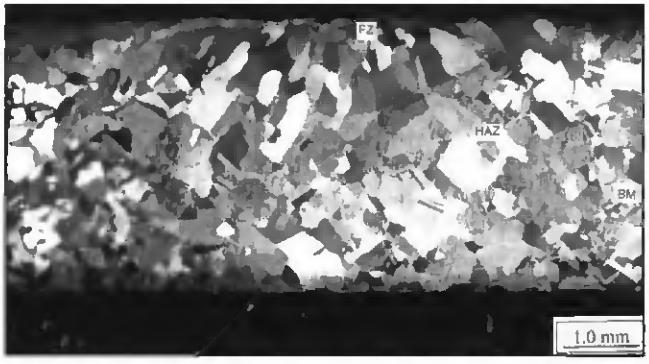

Fig. 6 — The shape of the fusion zone of a Ni-270 GTA weld at 5 g.

Results and Discussions

Figures 5–7 show photomacrographs of spot GTA welds performed on the MGRWS at accelerations of 1 (no rotation), 5 and 10 g, respectively. These macrographs are a cross section through the center of the weld fusion zone. To examine the effect of centrifugation on the weld fusion zone shape/profile, the depth and the width were measured, as outlined in the previous section. Table 3 shows the average depth, the average width and the average depth-to-width ratio of the fusion zone of the welds at various g levels. The data indicate that as g level (or rotation rate) increases, the average depth-to-width ratio of the weld fusion zones decreases (in the range of 1 to 10 g). To understand the reason for this trend of behavior, one should examine the controlling forces for an autogenous arc welding process during centrifugation. As was indicated earlier, Marangoni, electromagnetic and buoyancy are the dominant forces in an autogenous arc welding process at low arc currents. Once a metal is subjected to an arc welding process during centrifugation, not only does the buoyancy force increase, but also the Coriolis force is introduced in the weld pool of the form $2\omega \times v$, which in this case acts perpendicular to the plane of Fig. 4. The Coriolis acceleration does not necessarily influence the magnitude of the local fluid velocity, but it may alter the fluid flow pattern, which could affect the weld fusion zone shape. In this study, the effect of Coriolis force was not considered.

The effect of an increase in buoyancy acceleration in decreasing the d/w ratio of the weld fusion zone can be explained based on the three major forces; namely, the Marangoni, the electromagnetic and the buoyancy. Ni-270 has a negative surface tension gradient ($d\Upsilon/dT$) of -0.38×10^{-3} N/m°C, a reference density of 8900 kg/m^3 (Ref. 23) and a magnetic permeability of 0.251×10^{-3} H/m (Ref. 24). Observed from the top, for the case of Ni-270, the fluid flow pattern in the weld pool due to surface tension gradient (or Marangoni), the buoyancy and the electromagnetic are outward, outward and inward, respectively. Figure 8 shows the schematic of flow patterns due to Marangoni, buoyancy, electromagnetic and the overall resultant flow pattern. This figure shows an increasing buoyancy-driven flow results in a stronger outward flow, which results in an overall smaller inflow pattern and causes a shallower but wider weld fusion zone. This will decrease the depth-to-width ratio.

The relative importance between the surface-tension-driven flow and the buoyancy-driven

Table 3 — Average[a] d/w Ratio of the Weld Fusion Zone of Ni-270

g Level	Average Depth (d), mm	Average Width (w), mm	d/w Ratio
1.0	2.68	7.64	0.351
5.0	1.44	7.08	0.203
10.0	1.20	6.89	0.174

(a) Two welds per g level.

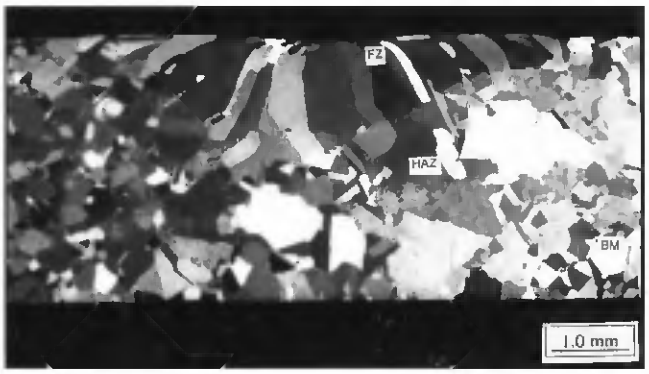

Fig. 7 — The shape of the fusion zone of a Ni-270 GTA weld at 10 g.

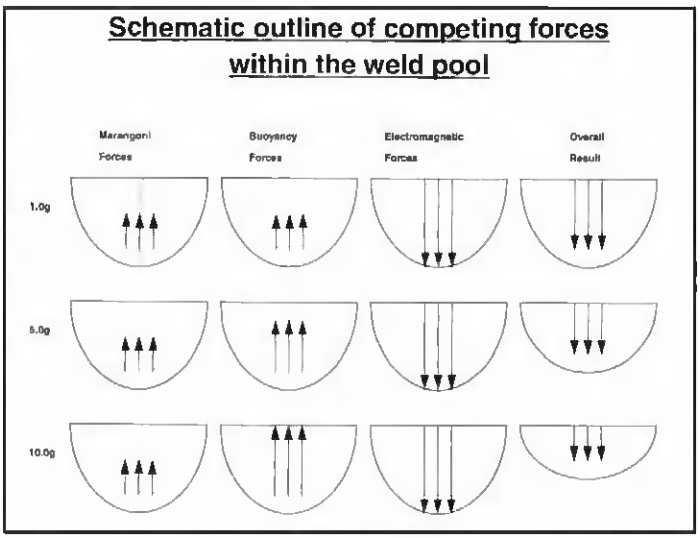

Fig. 8 — Schematic outline of the competing forces within the weld pool.

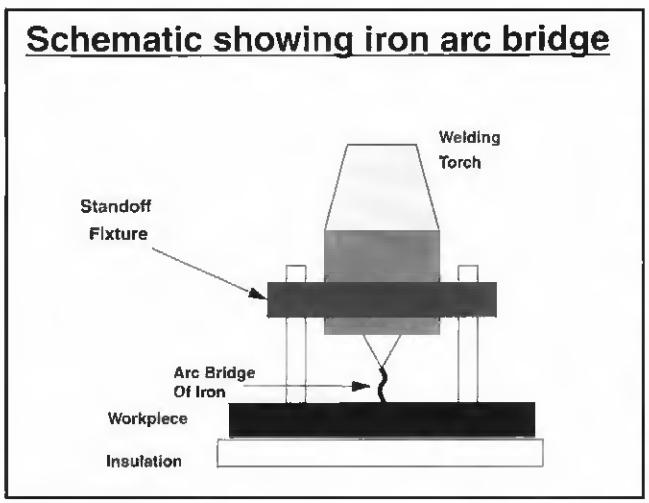

Fig. 9 — Schematic showing the addition of Fe to the Ni-270 weld pool.

Fig. 10 — The shape of the fusion zone of Ni-270 (with Fe) GTA weld at 1 g.

Fig. 11 — The shape of the fusion zone of Ni-270 (with Fe) GTA weld at 5 g.

Fig. 12 — The shape of the fusion zone of Ni-270 (with Fe) GTA weld at 10 g.

flow can be studied by examination of the Bond number (Bo). The Bond number, which is the ratio of buoyancy force to the surface tension force, is defined as $Bo = g\Delta\rho L^2/\gamma$, where g, $\Delta\rho$, L and γ, respectively, are the gravitational acceleration, change in density, characteristic length (1–3 mm) and surface tension (1.778 N/m) (Ref. 23). Using the appropriate values for each of the terms, the Bo numbers at 1 and 10 g are 0.29 and 2.9, respectively. These values of Bo number indicate that for this system (Ni-270), as the acceleration increases from 1 to 10 g, the buoyancy force becomes more significant than the surface tension.

The Atthey's number (At) is the ratio of the buoyancy force over the electromagnetic force (Ref. 25) and is defined as $At = g\Delta\rho/[\mu I^2/\pi^2 a^4]$, where μ, I and a are the magnetic permeability, the arc current (100 A) and the length scale (1–3 mm), respectively. Using the appropriate values for the terms, the At numbers at 1 and 10 g are 0.047 and 0.47, respectively. This dimensionless number shows that, even at 10-g acceleration, the electromagnetic force is stronger than the buoyancy force. Table 4 shows the relative magnitude of the three major forces for the Ni-270 weld. For this system, the electromagnetic force is the dominant force over the surface tension and buoyancy force even at 10 g. However, the net sum of the three forces as the g level increases results in a shallower and wider weld fusion zone, which decreases the depth-to-width ratio of the fusion zone.

To better visualize the shape of the spot GTA fusion zone of Ni-270 welds at various g levels, a trace element of iron (Fe, less than 0.01 grams) was added to the weld pool, as shown in Fig. 9. The addition of the Fe into the weld pool is the only parameter that was varied from previous welding experiments. Figures 10 through 12 show photomacrographs of the spot GTA welds of Ni-270 at 1, 5 and 10 g, respectively. The fusion zone in these macrographs is well defined. Table 5 shows the depth, the width and the depth-to-width ratio of the fusion zone of the spot GTA welds at various g levels. Figure 13 shows the depth-to-width ratio of the fusion zone as a function of g level with and without the trace element iron. These indicate that as the acceleration (g) increases the d/w decreases similarly to the welds without the trace element.

The shape of the fusion zone of the welds with the trace element indicates the fluid flow pattern was made of two opposing circulation patterns due to a maximum that exists in the γ-T relationship, as schematically shown in Fig. 14. In addition, the slope of d/w with the trace element is less than that without the trace element. These are due to the effect of added Fe on the three major forces that control the pattern of the convective flow in the weld pool mentioned earlier. It should be emphasized the addition of the trace of iron could have a significant effect on the electromagnetic and the surface tension of the weld pool. The addition of iron to Ni-270 changes the magnetic permeability of the weld pool, thus affecting the magnitude of the electromagnetic force but not the direction of the convective flow. It also changes the surface tension gradient of the weld pool surface, but it has a small effect on the buoyancy force. This is because the shape of the fusion zone in this case did not change as the g level increased.

What needs to be determined now is how significantly and in what way does the Coriolis force affect the overall convection pattern in the weld pool. Its significance is another interesting research topic. This, however, is left for a future study.

Table 4 — The Magnitude of the Forces (N/m^3) in the Ni-270 Weld Pool

Electromagnetic Force	9×10^5 N/m^3
Surface Tension	4×10^3N/m^3
Buoyancy force @ 1 g	1.2×10^4 N/m^3
Buoyancy force @ 10 g	1.2×10^5 N/m^3

Table 5 — Depth (d), Width (w) and d/w Ratio for Welds with Fe Addition

g level	d (mm)	w (mm)	d/w ratio
1 g	1.20	5.98	0.201
5 g	0.97	5.6	0.173
10 g	0.71	6.01	0.120

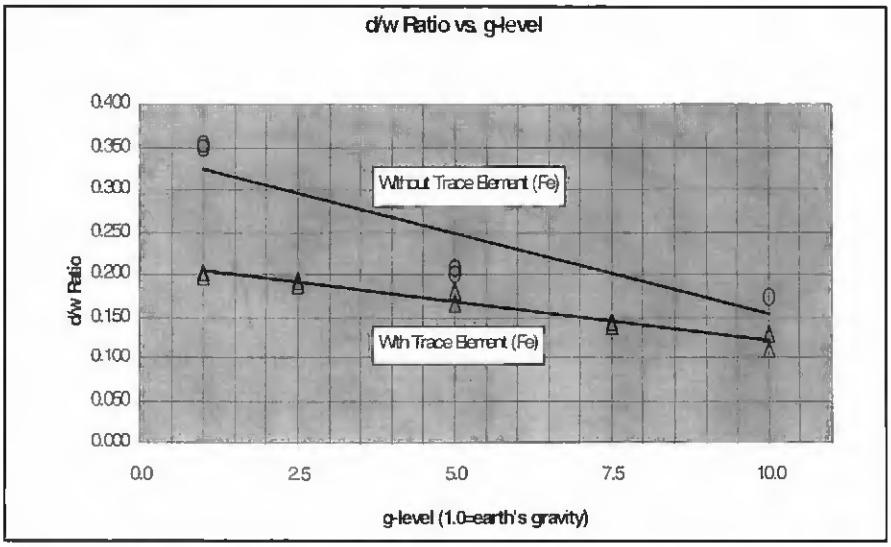

Fig. 13 — The depth-to-width ratio of the fusion zone of the Ni-270 with and without Fe addition vs. the g level.

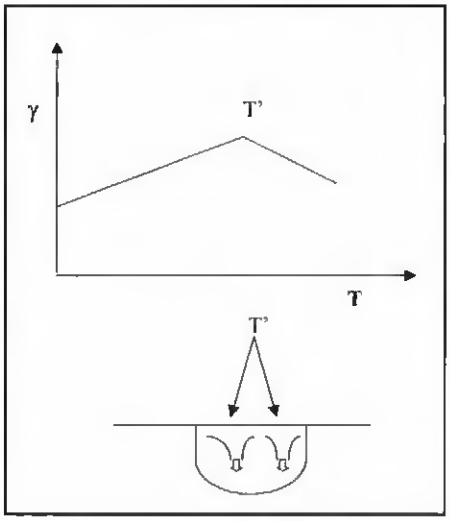

Fig. 14 — The fluid flow in the weld pool resulting from Marangoni convection (Heiple-Roper Theory) for the case of high levels of surface-active elements where a maximum exists in the γ-T relationship.

Conclusions

The present study shows the high gravity in the Ni-270 weld pool will noticeably reduce the depth-to-width ratio of the fusion zone. It is clear that an increase in buoyancy-driven flow induced by the high gravity will produce a wider, but shallower, weld fusion zone in metals such as Ni-270 with and without Fe as the trace element. It is conjectured that the addition of iron to Ni-270 produces a γ-T relationship similar to that shown in Fig. 14 that causes the two opposing flow patterns. This is because the addition of the trace of iron is not expected to significantly change the flow pattern due to electromagnetic and buoyancy forces.

References

1. David S. A., and DebRoy, T. 1992. Current issues and problems in welding science. *Science* 257: 497–502.

2. Kou, S., and Sun, D. K. 1985. *ASM Met. Trans. A* 16A (2): 203.

3. Kou, S. 1987. *Welding Metallurgy*. New York, N.Y., John Wiley & Sons, p. 91.

4. Correa, S. M., and Sundell, R. E. 1986. *Proceedings of the AIME Metallurgical Society.*

5. Oreper, G. M., Szekely, J., and Eager, T. W. 1986. The role of transient convection in the melting and solidification in arc weld pools. *ASM Met. Trans. B* 178: 735–744.

6. Chan, C. L., Mazumder, J., and Chen, M. M. 1987. *Material Science Technology*, 3.

7. Matsunawa, A., Yokoya, S., and Asako, Y. 1987. Trans. *JWRI*, 16.

8. Thompson, M. E., and Szekely, J. 1989. *Intl. Journal of Fluid and Mass Transfer*, 32.

9. Tsotridis, G., Rother, H., and Hondros, E. D. 1989. Marangoni flow and the shapes of laser-melted pools. *Naturwissensch* 76: 216–218.

10. Pardo, E., and Weckman, D. C. 1989. Prediction of weld pool reinforcement dimensions of GMA welds using finite-element model. *ASM Meta. Trans. B* 20B: 937–947.

11. Zacharia, T., David, S. A., Vitek, J. M., and DebRoy, T. 1989. Weld pool development during GTA and laser beam welding of type 304 stainless steel. *Welding Journal* 68(12): 499-s to 519-s.

12. Kim, S. D., and Na, S. J. 1992. Effect of weld pool deformation on weld penetration in stationary gas tungsten arc welding. *Welding Journal* 71(5): 171-s to 178-s.

13. Shirali, A. A., and Mills, K. C. 1993. The effect of welding parameters on penetration in GTA welds. *Welding Journal* 72(7): 347-s to 353-s.

14. Zacharia, T., Eraslan, A. H., and Aidun, D. K. 1988. Modeling of autogeneous welding process. *Welding Journal* 67(3): 53-s to 62-s.

15. Keanin, R. G., and Rubinsky 8. 1990. Plasma arc welding under normal and zero gravity. *Welding Journal* 69(6): 41–50.

16. Russel, C., Poorman, R., Jones, C., Nunes, A., and Hoffman, D. 1991. 23rd International SAMPE Technical Conference.

17. Kaukler, W. F., and Workman G. L. 1991. Welding in Space and the Construction of Space Vehicles. Welding technical conference.

18. Wang, G., and Tandon, K. N. 1993. The microstructure changes during laser welding of stainless steel under reduced gravity environment. *Microgravity Science Technology* VI/2.

19. Domey, J., Aidun, D. K., Ahmadi, G., Regel, L. L., and Wilcox, W. R. 1995. Numerical simulation of the effect of gravity on weld pool shape. *Welding Journal* 74(8): 263-s to 268-s.

20. Singh, J., Kang, N. H., Lambrakos, S. G., and Marsh, S. P. 1998. Gravity effects on the microstructural behavior and the development of weld pool. Microgravity Materials Science Conference. Huntsville, Ala.

21. Centrifuge designed for welding and casting in high Gs. 1997. News of Industry, *Welding Journal* (76)6: 18.

22. *Centrifugal Materials Processing*. 1997. L. L. Regel and W. R. Wilcox, eds. New York, N.Y., Plenum Press.

23. *Ullman's Encyclopedia of Industrial Chemistry*, 5th ed., Vol. A17. 1991. Cambridge, N.Y.

24. Kirk-Othmer. 1983, *Encyclopedia of Chemical Technology*, 3rd edition. New York, N.Y., John Wiley & Sons.

25. Atthey, D. R. 1980. *Journal of Fluid Mechanics* 98(4).